Effect of Structural Characteristics on Magnetic Behavior of Highly-Pure NiFe2O4 Nanoparticles

Sohaib Ahmed (sohaib.sabah@outlook.com)

University of Baghdad College of Education for Pure Science Ibn Al-Haitham https://orcid.org/0000-0001-5612-3411

Farouq I. Hussain

University of Baghdad College of Education for Pure Science Ibn Al-Haitham

Research Article

Keywords: Nickel ferrite, Ferromagnetic materials, Sol-gel, Magnetron sputtering

Posted Date: March 10th, 2021

DOI: https://doi.org/10.21203/rs.3.rs-300393/v1

Abstract

In this work, the sol-gel and dc reactive magnetron sputtering techniques were used to prepare nickel ferrite nanoparticles ($NiFe_2O_4$ NPs). In the sol-gel method, citric acid was used as a fuel to decompose metal complexes at a low temperature. The nanoparticle size of $NiFe_2O_4$ structures prepared by the dc reactive magnetron sputtering was smaller (~31 nm) than those prepared by the sol-gel method (~47 nm). The effects of the structural characteristics on the magnetic behavior of these nanoparticles were introduced by the vibrating sample magnetometer (VSM) measurements performed at room temperature. It was found that the nanoparticles synthesized by the sol-gel process exhibit ferromagnetic properties with a saturation magnetization 30.02 emu/g, while those synthesized by dc reactive magnetron sputtering exhibit superparamagnetic properties with a saturation magnetization of 27.05 emu/g. This difference is attributed to the quantum size effect resulted from the decrease in nanoparticle size.

1. Introduction

The field of nanotechnology has developed in the last few decades, especially in the physical sciences [1]. Many methods have emerged to produce nanomaterials, and these methods have a clear effect on the physical and mechanical properties of materials. These methods are divided into physical and chemical. Among the most important chemical methods is the sol-gel method, which is characterized by good chemical uniformity, high purity, crystallization, fine particle size, and simple equipment [2–4].

Physical vapor deposition (PVD) methods and techniques, such as plasma sputtering, pulsed-laser deposition (PLD), laser ablation, used for thin film deposition are mainly described as easy to assemble, reliable, very cheap, highly efficient, fast in performance and free of contaminations [5, 6].

Magnetic nanoparticles have important applications in color imaging, high-intensity recording, iron fluids, and magnetic refrigerators because of their unique properties. One of the most important uses of ceramic nanomaterials is to pass drugs to particular areas in the human body, alternative of radioactive materials utilized as tracers, and contrast agents in magnetic resonance imaging (MRI). Ferrites are the main component of magnetic ceramic materials. Among these ferrites, nickel ferrite ($NiFe_2O_4$) has distinctive properties for application as low-loss materials at high frequencies and soft magnets [5]. When the nanoparticles are small enough, the superparamagnetic behavior appears. Because Superparamagnetic nanoparticles have unique properties including their good colloidal stability, most importantly biological compatibility, high magnetization saturation, and high specific absorption rate (SAR) they are used in magnetic fluid hyperthermia (MFH) cancer therapy and magnetic resonance imaging (MRI) [7].

In this work, nickel ferrite ($NiFe_2O_4$) nanoparticles were prepared using two different methods: sol-gel and dc reactive magnetron sputtering. The differences in the structural characteristics and their effects on the magnetic behavior of the prepared nanostructures were studied.

2. Experimental Part

Nickel ferrite ($NiFe_2O_4$) nanomaterials were prepared by the sol-gel process by dissolving the citric acid ($C_6H_6O_7$) and the iron nitrate ($Fe(NO_3)_3.9H_2O$) in distilled water with continuous mixing with a magnetic stirrer. Hence, nickel nitrate ($Ni(NO_3)_2.6H_2O$) was added with a gradual increase in temperature. In order to make the solution neutral (pH), a few drops of ammonium hydroxide (NH_4OH) were added with continuous mixing, with the solution's density increasing clearly, the mixing was stopped and the temperature was fixed at 80 ℃. Then the solution turned into a gel (gel) and then bubbles increased and height in the beaker, and in the end, the mixture dried and became powdered from gray color. After that, the solution was burned at a temperature of 700 ℃ for two and a half hours with an increased rate of 5.6 ℃/min. The protocol of the sol-gel method used for preparation is shown in Fig. (1).

A dc reactive magnetron sputtering (DCRMS) system was used to prepare nickel ferrite nanoparticles. The deposition chamber was initially emptied down to 0.001 mbar by a rotatory pump while lower vacuum pressures (~ 10^{-5} mbar) could be reached by a diffusion pump. The first vacuum was limited by the scope of the removal process. Argon at the maximum pressure of 0.8 mbar was utilized as the removal gas and its pressure was finely regulated by the needle valve. During system operation, it is easy to change the inter-electrode distance from 0 to 10 cm. In order to prevent secondary electron emission, the cathode was cooled to 10 °C while the anode can be heated by an under heater or maintained at room temperature. The substrates on which films are deposited were placed on the surface of the anode, while the two highly-pure (99.99%) targets (Ni and Fe) were mounted on the surface of the cathode. To prepare a nickel ferrite compound, oxygen gas was used as reactive gas by mixing it with argon before pumped into the deposition chamber. More details on the DCRMS system and operation parameters can be found elsewhere [8–13].

After the deposition process, the nanomaterial was extracted as a powder from the thin films deposited on glass substrates by the conjunctional freezing-assisted ultrasonic extraction method [6]. This step would highly assist to determine the characteristics of the nanomaterial without any interference with the background from the substrate material.

The characterization and measurements included x-ray diffraction (XRD) patterns, field-emission scanning electron microscopy (FE-SEM), energy-dispersive x-ray spectroscopy (EDS), and vibrating sample magnetometer (VSM).

3. Results And Discussion

Figure (2) shows the diffraction patterns of the $NiFe_2O_4$ prepared by both methods: sol-gel and dc reactive magnetron sputtering. Distinguished peaks ascribed to the crystal planes (220), (222), (311), (400), (422), (440) and (511) were observed and they indicate the presence of cubic spinel $NiFe_2O_4$ structures in the prepared samples [14]. It is clear from these patterns that the nanoparticles prepared by

the sol-gel method (Fig. 2a) include sharp peaks, which reveal better crystallization when compared to the broadening observed in the patterns of the samples prepared by DCRMS [15].

The morphology of the prepared nanostructures was investigated by FE-SEM and those prepared by the sol-gel method reasonably include agglomeration while those prepared by DCRMS approximately have a spherical shape and uniform distribution. The nanoparticle size was determined to be within 33–62 and 22–40 nm for the samples prepared by sol-gel and dc reactive magnetron sputtering, respectively.

The elemental composition of the prepared $NiFe_2O_4$ samples was analyzed using EDS, as shown in Fig. (4). It was observed that the main components of the sample prepared by sol-gel are Fe, O, Ni, and C with 38.3, 19.3, 18.3, and 24 wt.%, respectively, as shown in Fig. (4a). On the other side, the elemental composition of the sample prepared by dc reactive magnetron sputtering showed the same elements Fe, O, Ni and C with the weight ratios of 37.5, 24.9, 23.2, and 13.5 wt.%, respectively, in addition to Mg of 0.9 wt.%. The increase of elemental contents of oxygen and nickel and decrease of carbon content in the second sample is highly preferred as the total content of $NiFe_2O_4$ is accordingly increased. The existence of carbon in the final product is unavoidable as the precursors in the sol-gel method include the availability of citric acid, which is the source of carbon while in the sputtering system, the possible source of carbon is using Teflon parts inside the deposition chamber. However, the content of carbon in the second sample is about half that in the first sample.

Figure (5) indicates the hysteresis loop of the synthesized $NiFe_2O_4$ nanostructures. The saturation magnetization (M_s) value in both methods is far lower from the recorded values for bulk nickel ferrite. The decrease in saturation magnetization is mainly attributed to the decrease in particle size [16]. The lower values of *Ms* associated with the crystalline nanoparticles ($NiFe_2O_4$) are due to the structural deformity of the surface as opposed to the bulk particles. This can be explained by the existence of transition metal ions to contain pure magnetic moment, which reacts through the oxygen atoms in the spinel lattice leading to a situation in which the magnetic moments of ions in the metal oxides forming the ferrite are aligned. The moments between the same metal oxide line up parallel, while the moments between different metal oxides are anti-parallel to result in a ferromagnetic order. By distributing metal ions to these sites, it is possible to calculate the net magnetic moment for each formula unit. Because the particles are very small, as the specimen has a large ratio of surface-to-volume, the net magnetic moment is decreased. Thus, on the surface of structural deformation particles, there is an availability of metal ions. The lengths and angles of the bonds are different when compared to the bulk to give low magnetic moments [17]. The saturation magnetization (M_s) and coercivity (H_c) of $NiFe_2O_4$ prepared by the sol-gel method are 30.02 emu/g and 187.8 Oe, respectively. Figures (5b) explains the typical behavior of the superparamagnetic behavior of the nanoparticles synthesized by DCRMS. It can be noticed that the saturation magnetization is 27.05 emu/g and the area of hysteresis is absent. This means that the coercivity is approximately zero. Because of the quantum size effect, the superparamagnetic behavior of the $NiFe_2O_4$ nanoparticles indicates that they have a single domain structure [18]. The superparamagnetic material in MRI in the absence of the applied magnetic field lose their magnetism, as

well as become highly dispersed in the liquid, making them suitable for cancer treatment in clinical treatments [19].

4. Conclusion

Two different methods: sol-gel and dc reactive magnetron sputtering, were used to prepare nickel ferrite nanoparticles. The second method showed the possibility to prepare samples with smaller nanoparticle size and higher structural purity. The magnetic behavior of the $NiFe_2O_4$ nanostructures prepared by dc reactive magnetron sputtering was superparamagnetic. These results would highly encourage to employ these nanostructures for developing instruments based on the magnetic properties of nanomaterials, such as MRI.

Declarations

Acknowledgment

Authors would like to thank people at Department of Physics, College of Science, University of Baghdad for their assistance in preparation of $NiFe_2O_4$ nanoparticles as well as people at Department of Physics, College of Education, Al-Iraqia University for their assistance in the extraction of nanopowders from the prepared samples.

Funding

Authors declare that this work was not funded or financially supported by any entity.

Conflict of Interest

Authors declare that they do not have any conflict of interest related to this work.

Data Availability

Authors confirm the availability of all data included in this manuscript as well as materials used for producing these data.

Code Availability

Authors declare that this work does not include any code.

Authors' contributions

SSA has carried out the experimental part, collected, classified and analyzed data and results, and prepared the draft of this manuscript.

FIH has analyzed the collected and classified data and results, and reviewed the draft of this manuscript.

References

1. Sagadevan, Z. Z. Chowdhury, and R. F. Rafique, “Preparation and Characterization of Nickel Ferrite Nanoparticles via Co-precipitation Method,” *Mater. Res.*, 21(2), 21–25, 2018.
2. Sutka and G. Mezinskis, “Sol-gel auto-combustion synthesis of spinel-type ferrite nanomaterials,” *Front. Mater. Sci.*, 6(2), 128–141, 2012.
3. M. El-Okr, A. Ashery, M. F. Zawrah, and A. B. A. Hammad, “Structural and Magnetic Analysis on Spinel $NiFe_2O_4$ Prepared by Sol Gel Process at Different Calcinations Temperatures Structural and Magnetic Analysis on Spinel $NiFe_2O_4$ Prepared,” *IOSR J. Appl. Phys.*, 8(3), 15–19, 2016.
4. Ramalho, M. A. F., et al. "Nanosize nickel ferrite particles synthesized by combustion reaction: evaluation of two synthesization routes." Materials science forum. Vol. 530. Trans Tech Publications Ltd, 2006..
5. George, A. Mary John, S. S. Nair, P. A. Joy, and M. R. Anantharaman, “Finite size effects on the structural and magnetic properties of sol-gel synthesized $NiFe_2O_4$ powders,” *J. Magn. Magn. Mater.*, 302(1), 190–195, 2006.
6. A. Hammadi, “Production of nanopowders from physical vapor deposited films on nonmetallic substrates by conjunctional freezing-assisted ultrasonic extraction method,” *Proc. Inst. Mech. Eng. Part N J. Nanomater. Nanoeng. Nanosyst.*, 232(4), 135–140, 2018.
7. Lee and T. Hyeon, “Designed synthesis of uniformly sized iron oxide nanoparticles for efficient magnetic resonance imaging contrast agents,” *Chem. Soc. Rev.*, 41(7), 2575–2589, 2012.
8. A. Hammadi, M.K. Khalaf, F.J. Kadhim, B.T. Chiad, “Operation Characteristics of a Closed-Field Unbalanced Dual-Magnetrons Plasma Sputtering System”, Bulg. J. Phys., 41(1) (2014) 24-33.
9. A. Hammadi, M.K. Khalaf, F.J. Kadhim, “Fabrication of UV Photodetector from Nickel Oxide Nanoparticles Deposited on Silicon Substrate by Closed-Field Unbalanced Dual Magnetron Sputtering Techniques”, Opt. Quantum Electron., 47(12) (2015) 3805-3813. DOI: 10.1007/s11082-015-0247-6
10. A. Hammadi, M.K. Khalaf, F.J. Kadhim, “Fabrication and Characterization of UV Photodetectors Based on Silicon Nitride Nanostructures Prepared by Magnetron Sputtering”, Proc. IMechE, Part N, J. Nanoeng. Nanosys., 230(1) (2016) 32-36.
11. A. Hammadi, M.K. Khalaf, F.J. Kadhim, “Silicon Nitride Nanostructures Prepared by Reactive Sputtering Using Closed-Field Unbalanced Dual Magnetrons”, Proc. IMechE, Part L, J. Mater.: Design and Applications, 231(5) (2017) 479-487.
12. A. Hammadi and N.E. Naji, “Characterization of Polycrystalline Nickel Cobaltite Nanostructures Prepared by DC Plasma Magnetron Co-Sputtering for Gas Sensing Applications”, Photon. Sens., 8(1) (2018) 43-47.
13. A. Hameed and Z.M. Jabbar, “Optimization of Preparation Conditions to Control Structural Characteristics of Silicon Dioxide Nanostructures Prepared by Magnetron Plasma Sputtering”, Silicon, 10(4) (2018) 1411-1418.

14. S. Singh and N. Sangwa, “Structural and Magnetic Properties of Nickel Ferrite Nanoparticles Synthesized by Ball Milling”, *Int. J. Eng. Sci. Invent.*, 6(10), 36–39, 2017.
15. Dormann, J. L., and D. Fiorani, eds. **“Magnetic properties of fine particles”**, Elsevier (Netherlands, 1992), p. 70.
16. H. Morr and K. Haneda, “Magnetic structure of small $NiFe_2O_4$ particles,” *J. Appl. Phys.*, 52(3), 2496–2498, 1981.
17. Huang and Z. Chen, “Nickel ferrite on silica nanocomposites prepared by the sol-gel method,” *J. Magn. Magn. Mater.*, 280(1), 37–43, 2004.
18. Srivastava, S. Chaubey, and A. K. Ojha, “Investigation on size dependent structural and magnetic behavior of nickel ferrite nanoparticles prepared by sol-gel and hydrothermal methods,” *Mater. Chem. Phys.*, 118(1), 174–180, 2009.
19. D. Thorat *et al.*, “Multimodal Superparamagnetic Nanoparticles with Unusually Enhanced Specific Absorption Rate for Synergetic Cancer Therapeutics and Magnetic Resonance Imaging,” *ACS Appl. Mater. Interfaces*, 8(23), 14656–14664, 2016.

Figures

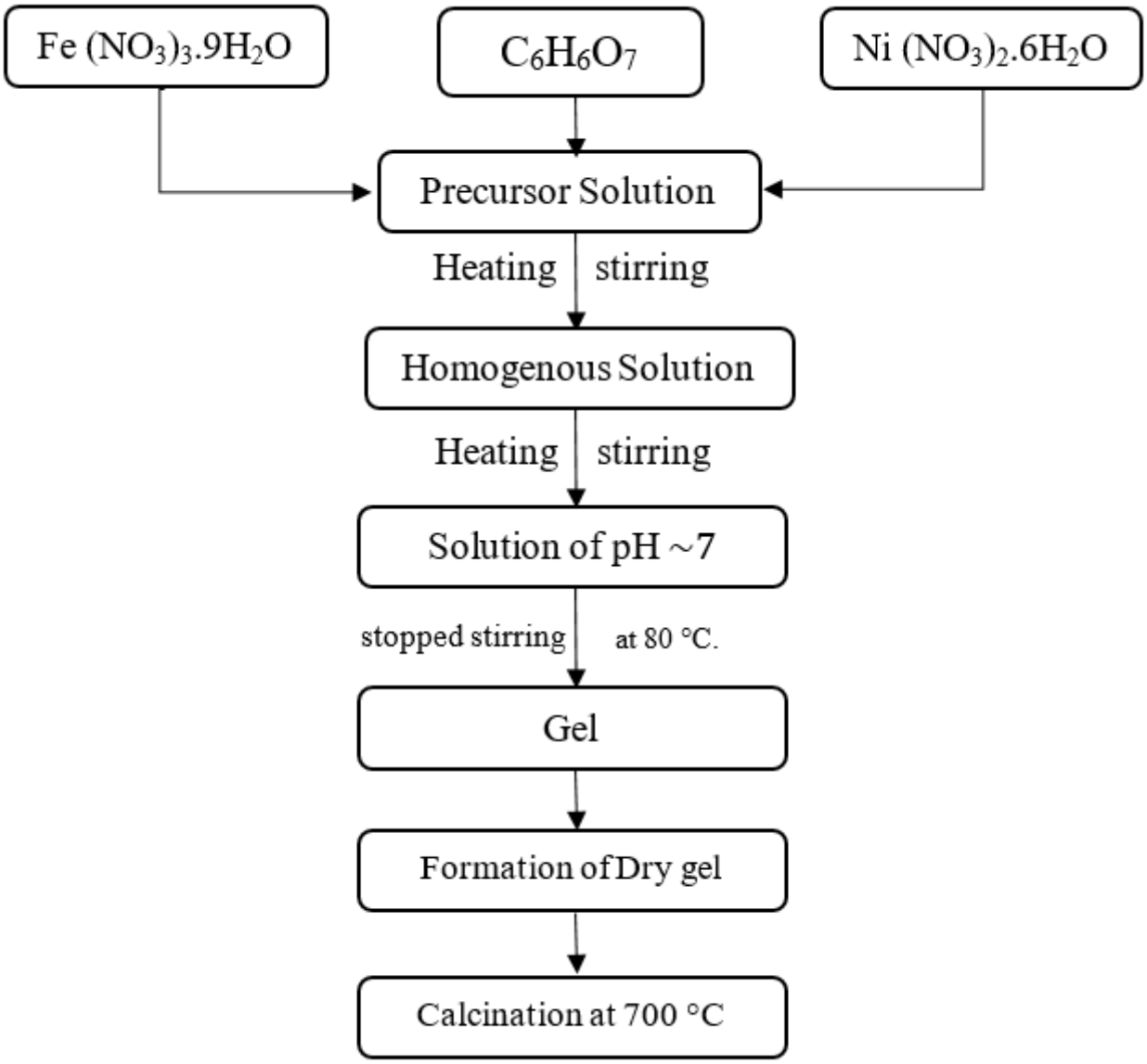

Figure 1

The protocol of sol-gel method

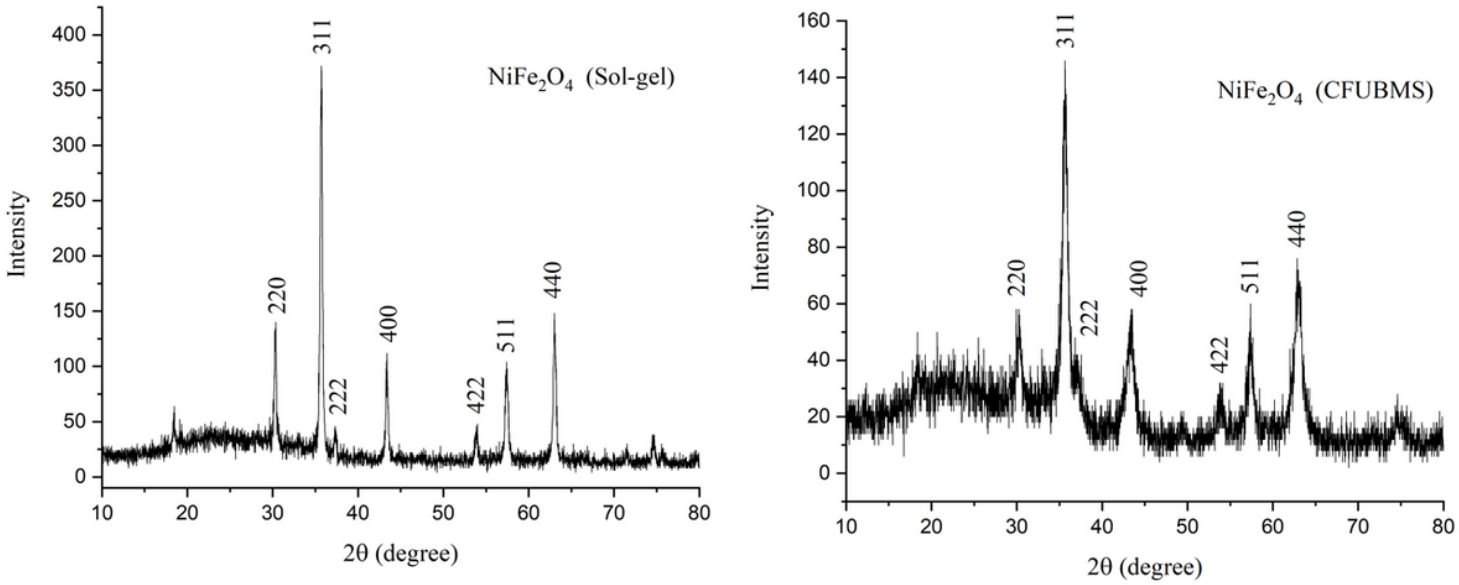

Figure 2

The XRD patterns of NiFe2O4 nanoparticles prepared by (upper) sol-gel and (lower) DCRMS

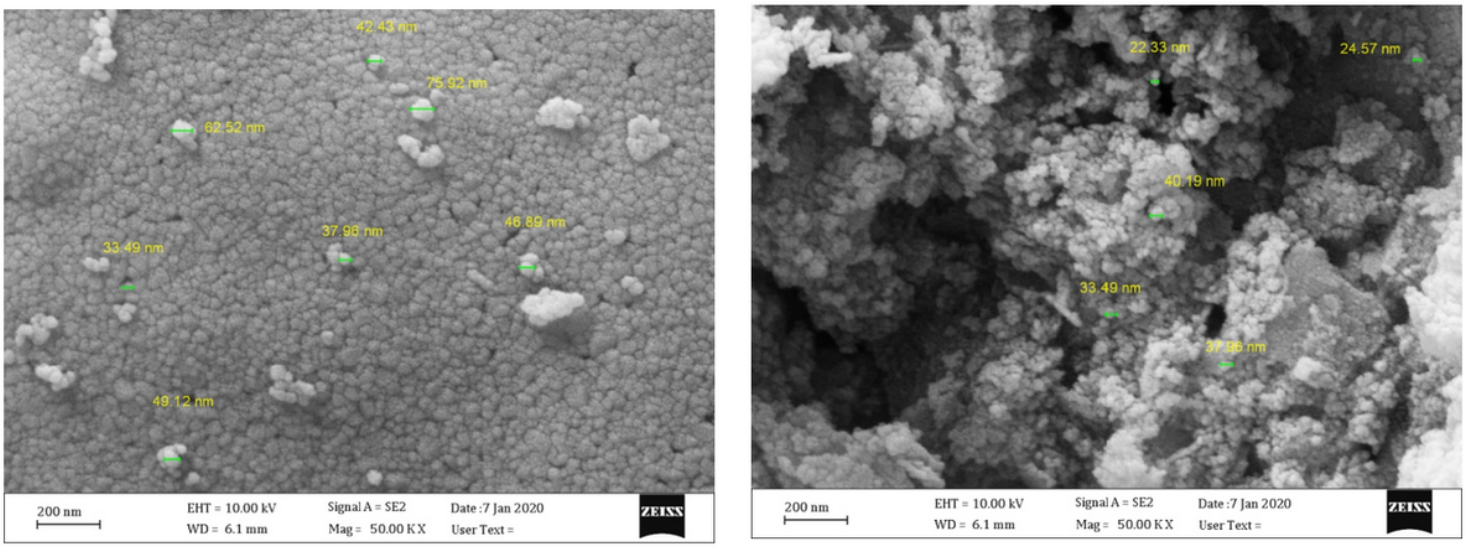

Figure 3

The SEM images of NiFe2O4 nanoparticles prepared by (a) sol-gel and (b) DCRMS

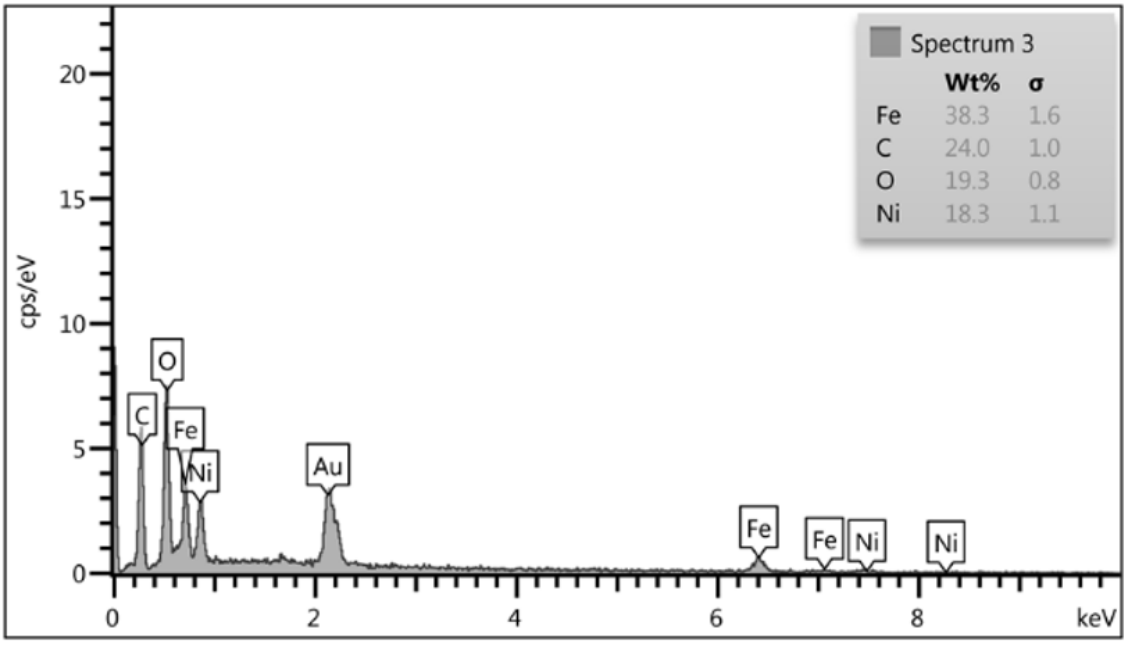

(a)

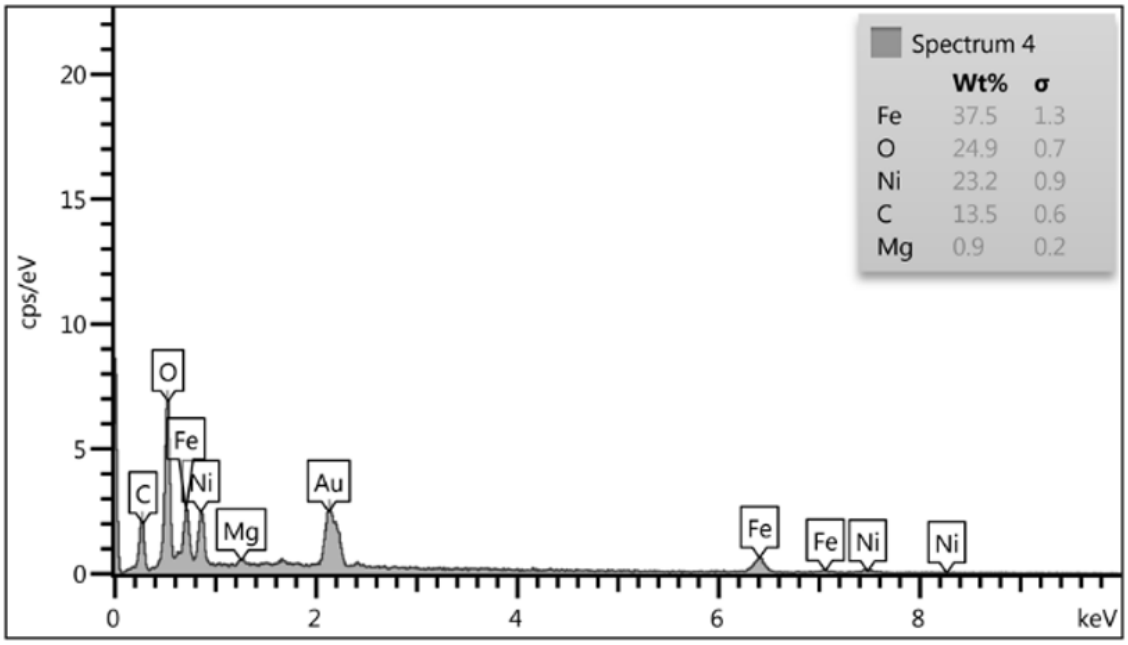

(b)

Figure 4

The EDS results of NiFe2O4 nanoparticles prepared by (a) sol-gel and (b) DCRMS

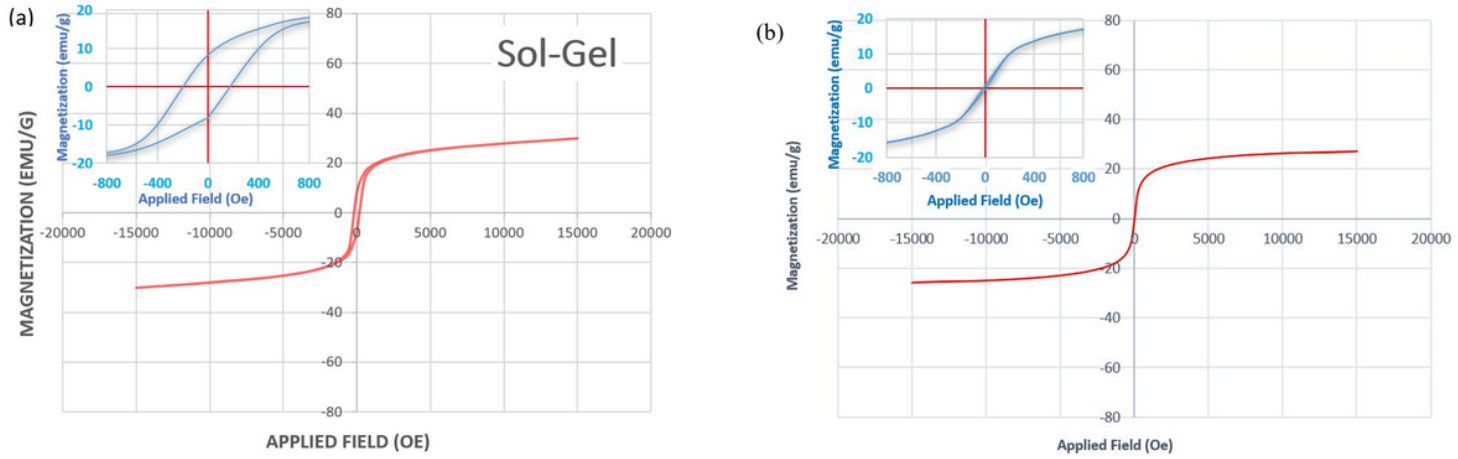

Figure 5

Hysteresis loop of NiFe2O4 nanoparticles prepared by (a) sol–gel and (b) DCRMS methods. The inset on the top in left corner is the part of the curve near the origin